A Streamlining Remote Sensing and Digitalization Process for Bridge Inspection

ZHENHUA SHI, HAIBIN ZHANG, TARUTAL GHOSH MONDAL, BRYAN A. HARTNAGEL and GENDA CHEN

ABSTRACT

One of the major challenges that prohibited the wide application of remote sensing photogrammetry in modern bridge inspection is the lack of advanced sensing platforms with a data analysis process. This study explores remote sensing for bridge inspection with a suite of unmanned aerial system (UAS) platforms accompanied by a follow-up digitization process for bridge inspection. To fully inspect a bridge of interest, a team of four complementary remote sensing UASs and equipment is employed, including a confined-space-specific Elios2 drone for bridge underdeck inspection, a DJI M600 equipped with LiDAR, thermal and hyperspectral sensors for above bridge deck sensing, an Anafi Parrot for side and above bridge deck RGB imaging, and a supplementary hand-held high-resolution camera for drone-inaccessible and high-priority areas. The digitized bridge inspection results cover multiple aspects of the bridge, including an interactive digital object represented by a dense point cloud, RGB images to reflect any visible surface deterioration (such as cracks, spalling, corrosion, and efflorescence), thermal images to reflect bridge deck near-subsurface delamination, and hyperspectral images to reflect any invisible bridge surface change. The digitized bridge model provides a comprehensive but intuitive digital representation of the inspected bridge. Compared to traditional bridge inspection practices with descriptive and subjective results, remote sensing photogrammetry shows great potential in efficient and consistent bridge inspection with fine details, which is believed to be necessary for reliable bridge condition assessment and long-term bridge health monitoring.

INTRODUCTION

Bridge inspection and maintenance play a significant role in modern bridge management, as an efficient and accurate assessment of the bridge condition is one of the cornerstones in maintaining the lifecycle of the modern highway transportation

Zhenhua Shi, Haibin Zhang, Tarutal Ghosh Mondal, Genda Chen*, Department of Civil, Architectural, and Environmental Engineering, Missouri University of Science and Technology, 500 W. 16th Street, Rolla MO 65409, USA.
Bryan A. Hartnagel, Missouri Department of Transportation, 105 W. Capitol Ave., P.O. Box 270, Jefferson City, MO 65102, USA.

system. The manual for bridge element inspection (MBEI) [1] provides a simple way to evaluate the condition of a bridge system. To categorize the bridge condition into one of four condition states (good, fair, poor, and severe), bridge inspectors need to describe the elements of the bridge and their quantities, the severity of the defects, and the service environment at the inspection time. However, the current engineering bridge inspection practice still relies on inspectors deployed on aerial work platforms (AWP) with simple tools such as tape measures, mirrors, cellphones, and notes, which presents several disadvantages such as high AWP maintenance costs, human-inaccessible areas, and traffic interruptions. Besides, the inspection deliverables typically are notes and cellphone images, which frequently results in subjective conclusions, making it difficult for bridge managers to make rational decisions.

On the other hand, UASs have been widely researched due to its potential to streamline the bridge inspection process and improve the consistency and accuracy of the deliverables. Zink and Lovelace [2] studied the potential advantages and challenges of using UASs to aid bridge inspection. Although only a military-grade Aeyron Skyranger [3] was studied, they concluded that UASs can be a great tool to aid bridge inspection. Wells and Lovelace [4] studied two UASs, including a senseFly Albris [5] and an Elios from Flyability [6], and focused on data postprocessing to improve the quality of the deliverables. Guo et al. [7] reported a streamlined bridge inspection framework to automatically identify the type, extent, and location of the defects. The authors validated the proposed framework on two bridges with three DJI drones, including Matrice600, Phantom4 Pro, and Mavic2 [8]. However, their inspection mainly focused on the side and above the bridge, and no inspection was performed underneath the bridge deck. Feroz and Dabous [9] provided a detailed review of the existing literature on this topic. Gordan et al. [10] briefly discussed the application of remote sensing and UAS in structural health monitoring (SHM) and provided a roadmap for future research. However, the scopes of the previous studies were limited in terms of inspection area, UAS type and sensing modality. There is no study, to the best of the authors' knowledge, provides a comprehensive guideline for holistic bridge inspection. This study aims to fill this knowledge gap by proposing a suite of heterogeneous UASs equipped with multimodal sensors for robotic bridge inspection with complete aerial coverage. Furthermore, although it has been observed that many state DOTs utilize UAS to inspect bridges, there is a lack of standardized protocol among the concerned agencies, this study also aims to address data inconsistency issue by creating a national-level cross-agency guideline for robotic inspection of bridges. In other words, this study incorporates the latest developments and state-of-the-art innovations in the fields of robotics and remote sensing to develop an intelligent bridge inspection protocol that seeks to replace the current manual practices, and to ensure consistency and reliability during data collection. Flight mission planning and representative data collection results are also presented.

UAS CHARACTERISTICS

Table I summarizes the characteristics and specific advantages of the selected UASs in terms of gimbal range, video/image resolution, maximum flight time, illumination capability, and obstacle avoidance availability. Presented UASs include Anafi Parrot [11], DJI M600 [8], and Elios2 from Flyability [6]. It should be noted here that the DJI

M600 carries a VLP-16 LiDAR from Velodyne [12], a FLIR Duo Pro R 640 thermal camera [13], and a hyperspectral sensor from Headwall [14], and the sensor lenses are fixed facing down. Figure 1 shows the images of the three UASs. Anafi Parrot is versatile for side and overall bridge inspection. It can also be used for bridge under-deck inspection with its unique 180° tilt gimbal capability if the transmission is not an issue at the bridge site. Elios2 is suitable for bridge under-deck inspection with its protection cage and illumination feature. It can be flown in bridge girder channels. Apart from that, a Nikon Coolpix P1000 [15] camera with 16 MP resolution, 125× optical zoom-NIKKOR ED glass lens, and 4K UHD/30fps is used for inspection in drone-inaccessible and high-priority areas.

The effectiveness of thermal imaging for concrete delamination detection was studied to interpret the inspection result from real-life bridges. Figure 2 shows the comparison between a thermal image and an RGB image from a mockup bridge (height: 2.13m) with embedded defects (size: 0.3m × 0.3m) generated by extruded polystyrene foamboards attached on plastic boards and placed alternately at the top and the bottom

TABLE I. CHARACTERISTICS OF UAS

UAS	Gimbal Range	Video/Image	Max. Flight Time	Illumination	Obstacle/Collision
Anafi Parrot	-90° to +90°	4K UHD /30fps, 21MP (4:3)	25 min	No	None
DJI M600 Pro	-90° (fixed)	Duo Pro R640, 640×512, 19mm, FOV 56°×45°	18 min (5.5 kg payload, TB48S batteries)	No	None
Elios2	-90° to +90°	4K/30fps, 12MP (4:3)	10 min	10K Lumens	Collision-Tolerant

(a) (b) (c)

Figure 1. UAS selected for bridge inspection (a) Anafi Parrot (b) DJI M600 Pro (c) Elios2

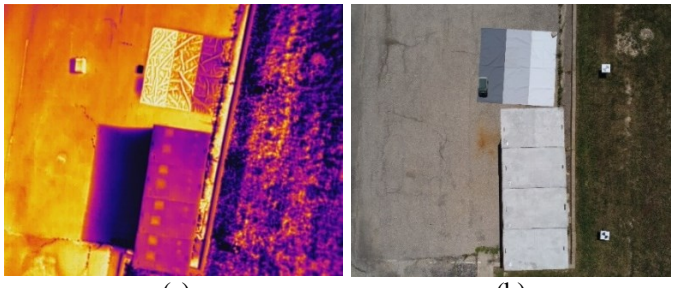

(a) (b)

Figure 2. Mockup bridge with embedded defects to study delamination detection effectiveness by thermal imaging (a) image from FLIR Duo Pro (b) image from Parrot drone

of the concrete slab having a concrete cover thickness of 2.54cm (1in) and 3.81 cm (1.5 in), respectively. The FLIR thermal sensor's height above ground level (AGL) can be calculated as 12.8m based on the size of the tarpaulin (3m × 3m) and the configuration of the sensor. The mockup bridge consisted of four concrete slabs, each having a size of 1.83m × 1.14m × 0.18m. The top embedded defects can be clearly seen from the thermal images but not on the regular RGB image collected by the Parrot drone, as shown in Figure 2(b). The defects on the bottom of the slab could not be detected due to deeper embedment. Therefore, thermal imaging effectively reveals shallow subsurface delamination of concrete structures. Note that a significant thermal difference on the target is necessary for the thermal detection to be effective, which means that the thermal imaging could only be conducted when a heating source such as sunlight or artificial heating is available.

FLIGHT MISSION PLANNING

A considerable amount of logistics is necessary before bridge inspection using UAS. Besides coordination with the state DOTs and compliance with FAA regulations [16], flight mission planning for bridge inspection using UAS also involves candidate bridge selection, flight crew establishment, flight path planning, and emergency plan establishment. Special permission from the Air Traffic Control (ATC) is required to inspect a bridge located outside a Class G airspace. A UAS flight crew should at least consist of a remote pilot in command (PIC) and a visual observer (VO). The PIC must complete recurrent training every 24 months after obtaining the remote pilot certificate. Drone operation training and practice are also necessary for those without prior experience, before operating on real bridges. All UASs must be registered with FAA if they are operated under part 107 category. An emergency plan also needs to be put in place to minimize any injury or property damage. In the event of a severe injury to any person, loss of consciousness, or damage to any property greater than $500 to repair or replace (whichever is lower), an accident report must be filed at FAA [16].

Figure 3 shows an autonomous flight path example for Missouri Bridge A4988 prepared in UgCS [17]. Planning the autonomous flight path takes into account the feature of interest and the minimization of direct flight over the traffic. The flight height is determined to avoid typical obstacles such as trees, powerlines, and utility poles. The flight height in Figure 3 is 40.5m AGL with a flight speed of 1.5m/s. The total number of waypoints is 16, with a total flight time of approximately 5min. Note that it is

Figure 3. Autonomous flight path with sensor-trigger polygon

recommended to have a safety factor (for example, 1.2) when designing the flight height, as the actual flight height may vary greatly from the design value. This is due to the low resolution of the digital elevation model (DEM) referenced as the ground elevation in the software. In the previous section of the mockup bridge study, the designed AGL flight height in UgCS is 16.2m, while the actual flight height is only 12.8m. The blueish lines in Figure 3 are the defined polygon where the hyperspectral sensor will be triggered, outside of which the sensor will be inactive. The flight path is designed along the wings of the bridge deck to minimize flying directly over the traffic. Depending on the maximum flight time of the UAS, the target resolution and specific bridge conditions (length, width, curvature, etc.), the flight height, path, and speed can be adjusted. The height is typically in the range of 30m-50m to overpass most obstacles and to minimize distractions to the traffic. The total flight time, which can be adjusted by flight speed and path, is usually kept within 15min (maximum: 18min) to have adequate time for a safe landing. For the flight paths underneath the bridge deck, Elios2 is flown in-between the girders to avert strong wind due to poor wind tolerance. Its collision-tolerance feature also comes in handy while navigating through narrow spaces. When it reaches the end of a span or the end of the entire bridge, the drone will be maneuvered into an adjacent girder channel and flown in the opposite direction. The flight path for bridge side inspection is to maintain a constant distance with the camera directly facing the bridge façade. A hand-held Nikon camera is used for drone-inaccessible areas such as bushy spans, dusty areas, tight space areas, and high-water level conditions.

CASE STUDY

This section presents the inspection data for Missouri steel bridge A4988 (total length: 109m, four spans: 21m + 31m + 31m + 26m), each having five steel girders. Figure 4 shows several representative images collected by the Parrot drone, which is suitable for the bridge side and overall inspection. Although only the images are presented here, the drone captures videos during data collection. Figure 4(a) shows the drone view when it was approaching the bridge after takeoff. Figure 4(b) shows the drone view on the bridge deck when it was flown near the side of the bridge. Figure 4(c) shows a captured image of the bolted connection of the steel girder, while Figure 4(d) shows the image captured near one of the bridge bents. Parrot was flown parallel to the bridge deck to capture features of interest such as bridge joints, pier bents, and any noticeable deteriorations. For bushy areas where flying drones would be risky, a hand-held camera would be used. Figure 5 shows several images taken from a Nikon camera, which can also be used for high-priority areas. Figure 5(a) shows the image captured of bolted connections on the steel girder from the bottom, while Figure 5(b) shows the captured side view from the bottom side of the bridge. Figure 5(c) shows the bottom view of the bridge deck with piers for the span over the trail, while Figure 5(d) shows the bottom of the bridge deck and piers for the span over the creek. The investigated bridge was 19 years old at the inspection time and was generally in good condition.

(a) (b) (c) (d)

Figure 4. Representative images taken from Parrot

(a) (b) (c) (d)

Figure 5. Representative images taken from Nikon camera

Figure 6 shows several representative images of the bridge taken from Elios2, which is designed for confined space inspection. The flight path for Elios 2 is to follow the girder channel to inspect the bridge girders, underneath the bridge deck, and the top of the bridge bents. No paint corrosion on the girders was noticed. Figure 7 shows the thermal images taken by the FLIR camera to reveal possible delamination at the subsurface. Specifically, Figure 7(a) shows the location at the approach span where the joints and road surface patches can be clearly noticed. Figures 7(b) and (c) show the thermal images for the approach span and middle span, respectively. Figure 7(d) shows the thermal image for the other approach span with a squared tarpaulin used for hyperspectral reflectance calibration. Abrasions can be noticed near the joints. No other major damage was noticed for the bridge decks.

(a) (b) (c) (d)

Figure 6. Representative images taken from Elios2 camera

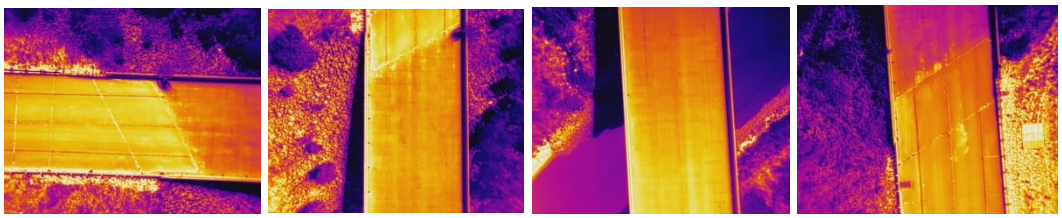

(a) (b) (c) (d)

Figure 7. Representative images taken from FLIR thermal camera

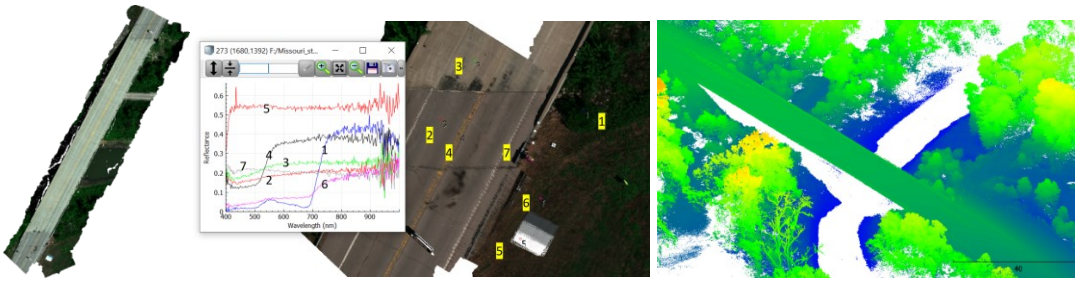

(a) (b) (c)

Figure 8. Data from Hyperspectral imaging (a) RGB-only overall view of the bridge (b) hyperspectral image of partial bridge (c) point cloud (unit: m)

Hyperspectral image contains continuous spectral information at each pixel and is useful for discrimination and characterization. The data is stored in a 3 dimensional hypercube (2 spatial + 1 spectral) which consists of a stack of images with wavelength information of the object. Figure 8(a) shows the hyperspectral image stitched together with only RGB bands for the Missouri bridge A4988, while Figure 8(b) shows a portion of the bridge with a continuous spectrum presented for each selected point of interest. Note that a high-capacity random access memory (RAM) computer is necessary as the hyperspectral image may be too large to be processed due to significant spectroscopic information contained at each pixel. Seven points were selected on the image, and distinctive spectra can be noticed. At the vegetation area (point 1), the spectrum jumps to near 720nm, while at the solid yellow traffic line (point 4), the spectrum jumps to near 540nm. The spectrum shows the highest reflectance at the white traffic line (point 5), starting from 460nm. The two different road surface materials also show a quite different reflectance. The darker asphalt area on the road (point 2) shows lower reflectance than the lighter concrete area on the bridge (point 3). The bluish guard rail (point 7) shows a gradual decrease starting from 460nm. The rusty area of point 6 shows a general increase from 680nm to 800nm. Therefore, hyperspectral sensing can distinguish close colors with abundant spectrum information. Figure 8(c) shows the point cloud in CloudCompare [18] generated from a Headwall LiDAR sensor. The feature of the tree can be noticed. The point cloud is generated as part of the research to digitize the bridge asset for long-term health monitoring. However, the point cloud is unavailable underneath the bridge deck since the drone with LiDAR sensor could not be flown underneath the bridge deck, which will be a part of future studies.

CONCLUSIONS

An end-to-end procedure has been presented for efficient and consistent bridge inspection using a suite of UASs, including Anafi Parrot, Elios2, Headwall DJI M600, and a Nikon camera. Complementary UASs are necessary to thoroughly inspect a bridge of interest as different UASs have different limitations. Anafi Parrot is suitable for overall and bridge side inspection, while Elios2 is suitable for confined spaces such as underneath the bridge deck and tunnel bridge inspection. Headwall UAS is suitable for RGB, thermal, and hyperspectral imaging from the top of the bridge deck with a predefined autonomous flight path. A high-resolution camera can be used in UAS-inaccessible areas and extreme operating conditions. Laboratory tests and a case study

on a Missouri steel bridge show that, complementary to RGB imaging, thermal imaging effectively reveals shallow subsurface delamination in bridge decks. In contrast, hyperspectral imaging is sensitive to any surface change with abundant spectral information. Additionally, a LiDAR point cloud can be generated for bridge asset digitalization. The presented procedure is believed to serve as a great reference for efficient and consistent bridge asset assessment and long-term health monitoring database establishment using UAS. Future studies may include defining autonomous flight paths for the side and underneath of bridge decks and developing LiDAR solutions for GPS-denied areas such as underneath of bridge decks and tunnel bridges.

ACKNOWLEDGEMENT

Funding for this research is provided by the Transportation Pooled Fund Program Project #TPF-5(395). The authors also appreciate the support from the Missouri Department of Transportation for field studies. The views, opinions, and conclusions reflected in this paper are solely of the authors and do not represent the official policy or position of the sponsors.

REFERENCES

1. American Association of State Highway and Transportation Officials (AASHTO). Manual for bridge element inspection, 2nd Edition (2019).
2. Jennifer Zink, Barritt Lovelace. Final Report, MN/RC 2015-40. Unmanned Aerial Vehicle Bridge Inspection Demonstration Project (2015).
3. Aeyron Skyranger Homepage, https://www.aerocontact.com/en/virtual-aviation-exhibition/product/98-UAS-skyranger, last accessed 2023/05/08.
4. Jennifer Wells, Barritt Lovelace. Final Report, MN/RC 2018-26. Improving the Quality of Bridge Inspections Using Unmanned Aircraft Systems (UAS) (2018).
5. SenseFly Albris. Brochure, https://www.sensefly.com/app/uploads/2018/05/albris_EN.pdf.
6. Elios Homepage, https://www.flyability.com/, last accessed 2023/05/08.
7. Yanlin Guo, Brandon J. Perry, Rebecca Atadero, John W. van deLLindt. Final Report, MPC-535, MPC-592 (combined). A streamlined bridge inspection framework utilizing unmanned aerial vehicles (UASs) (2021).
8. DJI Homepage, https://www.dji.com/, last accessed 2023/05/10.
9. Feroz, S.; Abu Dabous, S. UAS-Based Remote Sensing Applications for Bridge Condition Assessment. Remote Sens. (2021)13, 1809. https://doi.org/10.3390/rs13091809.
10. Meisam Gordan, Zubaidah Ismail, Khaled Ghaedi, Zainah Ibrahim, Huzaifa Hashim, Haider Hamad Ghayeb, Marieh Talebkhah. A Brief Overview and Future Perspective of Unmanned Aerial Systems for In-Service Structural Health Monitoring. Engineering Advances, 1(1), 9-15. DOI: 10.26855/ea.2021.06.002 (2021).
11. Anafi Parrot Homepage, https://www.parrot.com/us/drones/anafi/technical-specifications, last accessed 2023/05/08.
12. Velodyne Lidar Homepage, https://velodynelidar.com/products/, last accessed 2023/05/08.
13. Teledyne FLIR Homepage, https://www.flir.com/support/products/duo-pro-r/#Overview, last accessed 2023/05/08.
14. Headwall Photonics Homepage, https://www.headwallphotonics.com/, last accessed 2023/05/08.
15. NikonUSA Homepage, https://www.nikonusa.com/en/nikon-products/product/compact-digital-cameras/coolpix-p1000.html, last accessed 2023/05/10.
16. Federal Aviation Administration UAS Homepage. https://www.faa.gov/uas/, last accessed 2023/05/08.
17. UgCS Homepage, https://www.ugcs.com/, last accessed 2023/05/08.
18. CloudCompare, Version 2.13 alpha, https://www.cloudcompare.org/.